Performance of CO_2 adsorption by hybrid amine-functionalized MCM-41

Zhoubing Cheng[a], Qunpeng Cheng[b,*]

[a]*Office of Construction and Campus Planning, China University of Geosciences (CUG), Wuhan, Hubei 430074, China, email: chengzhoubing@163.com*
[b]*School of Chemical and Environmental Engineering, Wuhan Polytechnic University, Wuhan, Hubei 430023, China, email: cqp627@126.com*

ABSTRACT

In this study, the performance of modified MCM-41 adsorbents by impregnation and grafting modification with 3-aminopropyltriethoxysilane (APTS) and polyethyleneimine (PEI) on the CO_2 adsorption was investigated. The results showed that the synergistic effect of APTS and PEI could improve the adsorption performance and thermal stability of the MCM-41 adsorbents. The CO_2 adsorption capacity of mixed amine-modified MCM-41 adsorbents was higher than single amine modified MCM-41 adsorbents. The maximum adsorption capacity (2.6512 mmol g^{-1}) was obtained at MCM-41-APTS-5%-PEI-50%. Meanwhile, the adsorbents modified by mixed amine showed good cycle regeneration stability after five times of CO_2 adsorption/desorption cycling.

Keywords: Mixed amine; Mesoporous silicon; Two-step methods; CO_2 adsorption

1. Introduction

The rapid development of industry has led to a sharp increase on the concentration of CO_2 in the atmosphere, resulting in a series of global environmental problems like global warming [1]. Therefore, it is urgent to develop efficient CO_2 capture technologies to control CO_2 emission.

Currently, CO_2 capture technologies mainly include liquid absorption [2,3], membrane separation [4,5] and solid phase adsorption [6,7], etc. While for liquid absorption, the absorbent is easy to be oxidized under the condition of oxygen, and the regeneration of absorbent is large energy consumption. The process of membrane separation is very complicate which needs gas separation for dehydration, filtration and other pretreatments. Using recycled solid adsorbent for the CO_2 capture can effectively overcome the shortcoming of liquid absorption and membrane separation, which has the advantages of low energy consumption, stable performance and simple operation [8,9].

Commonly used solid adsorbents are mainly natural zeolite [10,11], molecular sieves [12,13], activated

alumina [14], silica gel [15] and activated carbon [16–18], etc. While those traditional adsorbents usually have poor selectivity due to interference of other gases, or the adsorption capacity can be greatly affected by the temperature. Mesoporous silica materials represented by MCM-41 and SBA-15 is widely used for CO_2 adsorption due to its regular honeycomb pore structure, huge pore volume, high specific surface area (up to 1,000 m^2 g^{-1}), and easy to be prepared in industrialization [19–25]. However, simple mesoporous silica materials have low adsorption capacity and poor selectivity for CO_2 [26]. In order to improve its CO_2 adsorption performance, amino functional groups are usually introduced [27,28]. Amino functional groups can be introduced by two ways: impregnation method and grafting method. The impregnation method is a physical loading method, which relies on van der Waals forces to connect organic amines to the carrier. Wei et al. [29] found that the CO_2 adsorption capacity of MCM-41 impregnated by triethylenetetramine (TETA) had the highest adsorption capacity of 2.22 mmol g^{-1} at 60°C,

---

* Corresponding author.

compared with MCM-41 impregnated by diethylenetri-amine (DETA), TETA and 2-amino-2-methyl-1-propanol (AMP) [29]. While a maximum CO_2 adsorption capacity of 2.7 mmol g⁻¹ was achieved on MCM-41 impregnated with tetraethylenepentamine (TEPA) with 40% TEPA [30]. Van der Waals forces between amine group and the carrier are weak which results in a low thermal stability of the adsor-bent. Amine group can easily be detached from the carrier resulting in the decrease of adsorption activity. It is differ-ent from impregnation method, amine can be loaded by chemical bonds by the grafting method which results in a strong thermal stability [31,32]. In addition, amine can be well dispersed on the surface of the carrier by grafting method which results in a fast adsorption rate compared with impregnation method [33]. However, the amount of amine is limited by grafting method which results in a lower adsorption capacity. In order to improve the adsorp-tion performance and thermal stability of the adsorbents a two-step method (grafting followed by impregnation) was proposed [34]. It was found that with the increase of tem-perature, the CO_2 adsorption capacity of amine-function-alized mesoporous materials was increased. Meanwhile, the adsorption capacity of amine-modified materials by two steps was stronger than that of amine-modified materials by single step. The adsorbents also displayed an excellent stability and renewability.

The CO_2 adsorption capacity of the adsorbents is not only influenced by the type of amines but also by the mod-ification methods. While many researches were focused on immobilizing the liquid amine in the MCM-41 by the impregnation or grafting method, few researches com-bining the two methods were studied. Hence, a two-step method combining impregnation and grafting modifica-tion with 3-aminopropyltriethoxysilane (APTS) and poly-ethyleneimine (PEI) was developed to modify the MCM-41 adsorbents in this study. The adsorption performance of the MCM-41 adsorbents under different loading rates was comprehensively studied. Meanwhile, the CO_2 absorption/desorption cycle experiment was carried out to evaluate thermal stability and regeneration performance. This paper will provide useful guidance for the CO_2 capture.

2. Materials and methods

2.1. Preparation of MCM-41-APTS-x-PEI-y adsorbents

Aqueous ammonia (25%, analytical reagent) and anhy-drous ethanol was purchased from Damao Chemical Reagent Factory (Tianjin, China); cetyltrimethylammonium bro-mide (CTAB) and tetraethyl orthosilicate (TEOS) came from Sinopharm Chemical Reagent Co., Ltd., (Shanghai, China). PEI and APTS were obtained from Aladdin Chemistry Co., (China).

MCM-41 was synthesized according to the literature [31]: 55.54 g 25% aqueous ammonia, 2.19 g cetyltrimeth-ylammonium bromide (CTAB) and 75.35 g distilled water were added into a polytetrafluoroethylene bottle and stirred for 30 min. Then 10.42 g tetraethyl orthosilicate (TEOS) was added dropwise. The solution was hold at 80°C for 96 h. After cooled down, it was filtrated and washed until no foam observed. After dried at 80°C, MCM-41

products were obtained by calcination at 550°C for 5 h. The MCM-41-APTS-*x*-PEI-*y* adsorbents were prepared by two steps: grafting and impregnation.

- APTS grafting: MCM-41 was modified with APTS by the grafting method using the procedure reported in the literature [31]. 1 g of MCM-41 was stirred in 100 mL anhydrous ethanol for 10 min. Then, the desired amount of APTS was added drop by drop and the slurry was stirred and refluxed for 10 h at 70°C. The APTS-modified adsorbent (denoted as MCM-41-APTS-x) was obtained after washing with anhydrous ethanol repeatedly and drying at 80°C for 12 h. *x* stands for the loading rate of APTS (3, 5, 7, 10, 20, 30 and 40 wt.%).
- PEI impregnation: MCM-41-APTS-x was modified with PEI by the impregnation method using the follow-ing procedure reported in the literature [31]. Certain amount of PEI was dissolved in 20 mL anhydrous etha-nol and stirred for 10 min. Then, 1.0 g MCM-41-APTS-x was added to the solution. The slurry was continu-ously stirred for 8 h at room temperature, and the PEI-modified adsorbent (denoted as MCM-41-APTS-*x*-PEI-*y*) was obtained by drying at 80°C for 12 h. y stands for the loading rate of PEI (30, 40 and 50 wt.%).

2.2. Characteristic of adsorbent

The chemical composition of the adsorbents was deter-mined by X-ray diffraction (ASAP 2020, USA). Nitrogen adsorption–desorption was carried out by using an auto-matic specific surface aperture distribution analyzer (AUTOSORB-6B, USA) and the specific surface area and pore-size distribution were calculated by using Barrett–Joyner–Halenda (BJH) method. The functional groups of the adsorbents were tested by Fourier-transform infrared spec-troscopy (FT-IR) (Nicolet is10, USA). Thermogravimetric analysis (TGA) for the adsorbents was carried out in a ther-mogravimetry and differential thermal analysis (TG/DTA) instrument (SDT Q600, TA Instruments).

2.3. CO_2 adsorption performance of adsorbents

The schematic diagram of the CO_2 adsorption appa-ratus is shown in Fig. 1. The CO_2 adsorption capacity (*q*, mmol g⁻¹) could be calculated according to Eq. (1) [31]:

$$q = \frac{\dfrac{m_2 - m_1}{M} \times 1,000}{m_1 - m_0} \tag{1}$$

where M is the molecular weight of CO_2; m_0 is the mass of the empty U-shaped tube; m_1 is the mass of U-tube and adsorbent before adsorption; m_2 is the mass of U-tube and adsorbent after adsorption.

3. Results and discussion

3.1. Characterization of MCM-41-APTS-x-PEI-y adsorbents

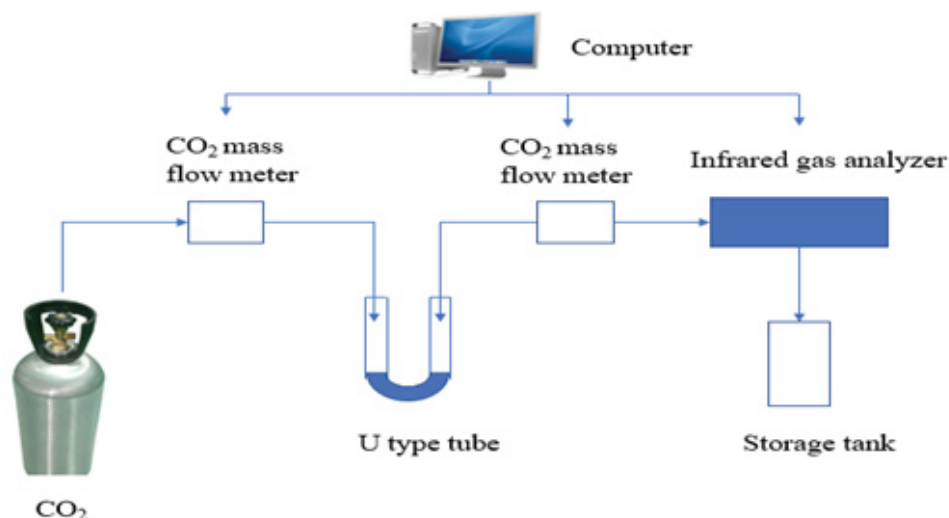FT-IR spectra of amine-modified adsorbents are dis-played in Fig. 2. The peaks at 587, 1,025, and 790 cm⁻¹ were

Fig. 1. Schematic diagram of CO_2 adsorption apparatus.

characterized by bending vibration peak, symmetric and asymmetric stretching vibration peak of Si–O–Si respectively [34,35], which indicated that the mesoporous structure of MCM-41 was not changed after APTS and PEI modified. Compared with MCM-41, the peak at 1,560 cm^{-1} was the bending vibration of N–H bond which was caused by the loading of APTS and PEI [36]. It indicated that APTS and PEI were successfully loaded into the channel of MCM-41. Meanwhile, with the increase of APTS loading rate, the peaks at 1,560, 1,460 and 2,985 cm^{-1} in MCM-41-APTS-*x*-PEI-30% represented for bending vibration of N–H bond, bending vibration and stretching vibration of C–H bond became stronger.

The TGA curves of MCM-41-APTS-*x*-PEI-*y* adsorbents were shown in Fig. 3. The weight loss appeared at 100°C was caused by the volatilization of water and residual solvent in the preparation process. The adsorbents were completely decomposed at 600°C. A significant weight loss could be observed in the 100°C–400°C with a total weight loss of 26.25%, 30.97% and 37.64%, respectively for MCM-41-APTS-5%-PEI-30%, MCM-41-APTS-5%-PEI-40% and MCM-41-APTS-5%-PEI-50%, which indicated that the thermal stability of adsorbents was increased with the loading of PEI. Meanwhile, the initial amine decomposition temperatures of MCM-41-APTS-5%-PEI-30%, MCM-41-APTS-5%-PEI-40% and MCM-41-APTS-5%-PEI-50% were 270°C, 260°C and 250°C respectively. It was higher than that of adsorbents prepared by the PEI impregnation (150°C) and APTS grafting (150°C), which indicated that the thermal stability of adsorbents could be improved by two steps [31]. The weight loss could be divided into two stages in the 100°C–400°C range which was similar to the results of previous work. The difference was the temperature distribution of weight loss where a slow weight loss
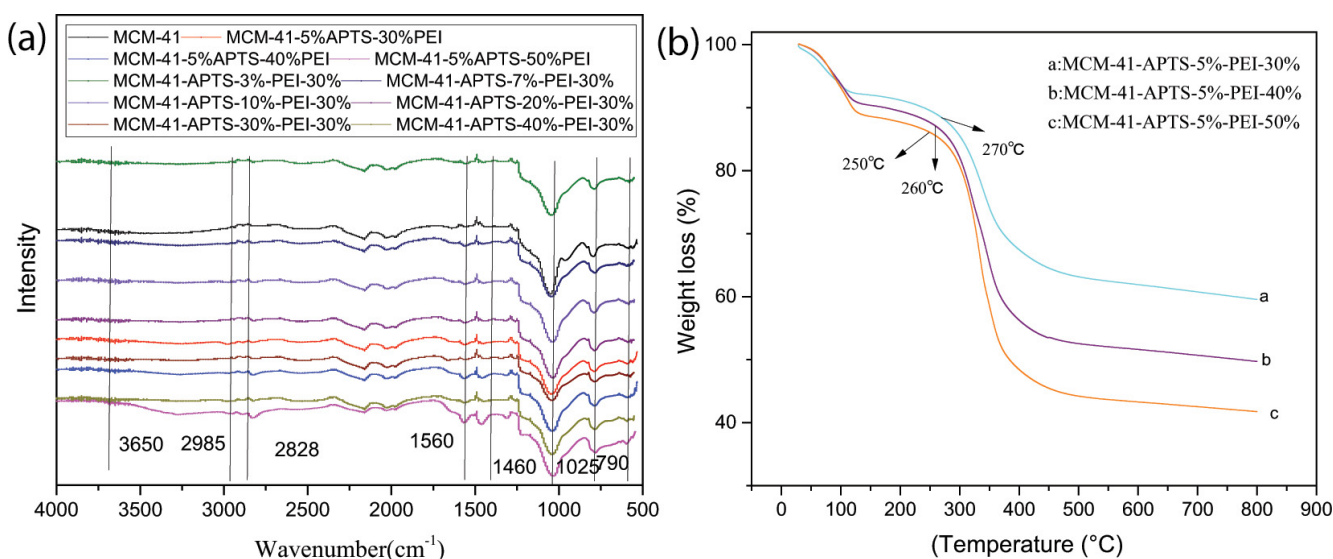

Fig. 2. Characteristic of adsorbents: (a) FT-IR spectra and (b) TGA curve.

Table 1
Structural properties of adsorbents

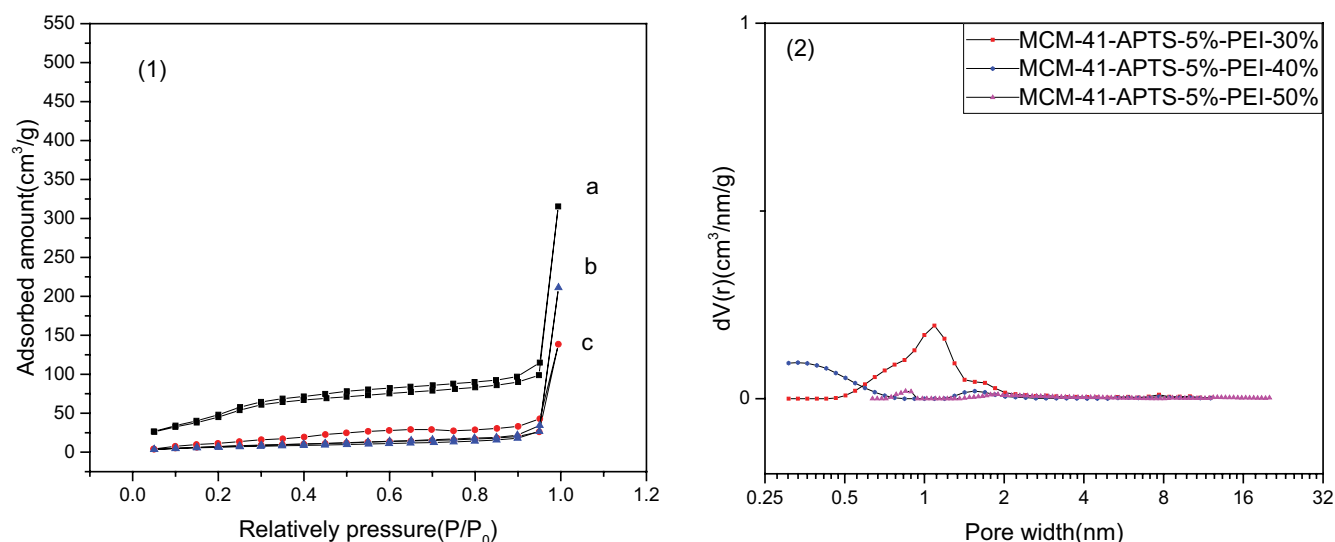| Adsorbents	Brunauer–Emmett–Teller surface ($m^2 \ g^{-1}$)	Pore volume ($cm^3 \ g^{-1}$)
MCM-41-APTS-5%-PEI-30%	196.912	0.167
MCM-41-APTS-5%-PEI-40%	31.34	0.061
MCM-41-APTS-5%-PEI-50%	25.476	0.05

Fig. 3. Nitrogen adsorption–desorption isotherm (1) and pore-size distribution (2): (a) MCM-41-APTS-5%-PEI-30%, (b) MCM-41-APTS-5%-PEI-50%, and (c) MCM-41-APTS-5%-PEI-40%.

stage occurred in the 100°C–250°C and a fast weight loss stage occurred in the 250°C–400°C. APTS not only reacted with the silicon hydroxyl in the MCM-41 channel during the grafting process and caused the space separation, but also introduced some amino and hydroxyl in the channel and supplied the site space and hydrogen bond connections for the evenly disperse and fix of PEI, which increased the initial PEI decomposition temperature. Moreover, the adsorbent prepared remained stable below 150°C, indicating that it could be recycled for adsorption/desorption.

3.2. N₂ adsorption–desorption isotherms

The nitrogen adsorption–desorption isotherm and pore-size distribution of adsorbents are shown in Fig. 4(1) and (2). The adsorption isotherm of adsorbents presented type IV and H4 type hysteresis loop after the modification by APTS and PEI, indicating that the adsorbents were mesoporous. With the increase of loading rate, the pore volume of the adsorbents was decreased gradually, resulting in the gradual decrease of its hysteresis loop. Among them, MCM-41-APTS-5%-PEI-50% had a narrow hysteresis loop, indicating that the holes of MCM-41 carrier were not all filled. While if there was no hysteresis loop, it indicated that the channel of MCM-41 carrier had been blocked.

As could be seen from the aperture distribution (Fig. 4), the average pore radius and the average pore diameter of MCM-41 was 1.3 and 2.6 nm. The average

pore radius and the average pore diameter of MCM-41-APTS-5%-PEI-30% were 1.0915 and 2.182 nm. The average pore radius and the average pore diameter of MCM-41-APTS-5%-PEI-40% were 0.333 and 0.666 nm. The average pore radius and the average pore diameter of MCM-41-APTS-5%-PEI-50% were 0.8485 and 1.696 nm. The pore volume of these adsorbents was decreased with the increase of PEI load. According to the structural properties of adsorbents in Table 1, the specific surface area and pore volume of modified MCM-41 materials were decreased with the increase of PEI loadings, which was attributed to the coverage of PEI on the MCM-41 [37].

3.3. Adsorption performance

The CO_2 adsorption capacities of adsorbents are shown in Fig. 5. Compared with MCM-41 (0.75 mmol g^{-1}) in the literature [31], the adsorption capacity of adsorbents had been greatly improved after modification. When the loading amount of APTS was less than 5 wt.%, the adsorption capacity of the adsorbents was gradually increased with the PEI loading amount. The increase of PEI loading amount resulted in an increase of amino active sites reacting with CO_2. While when the loading amount of APTS was larger than 7 wt.%, the adsorption capacity of the adsorbents was gradually decreased with the PEI loading amount, and with the increase of APTS loading amount, the adsorption capacity was become small. Excessive loading of APTS
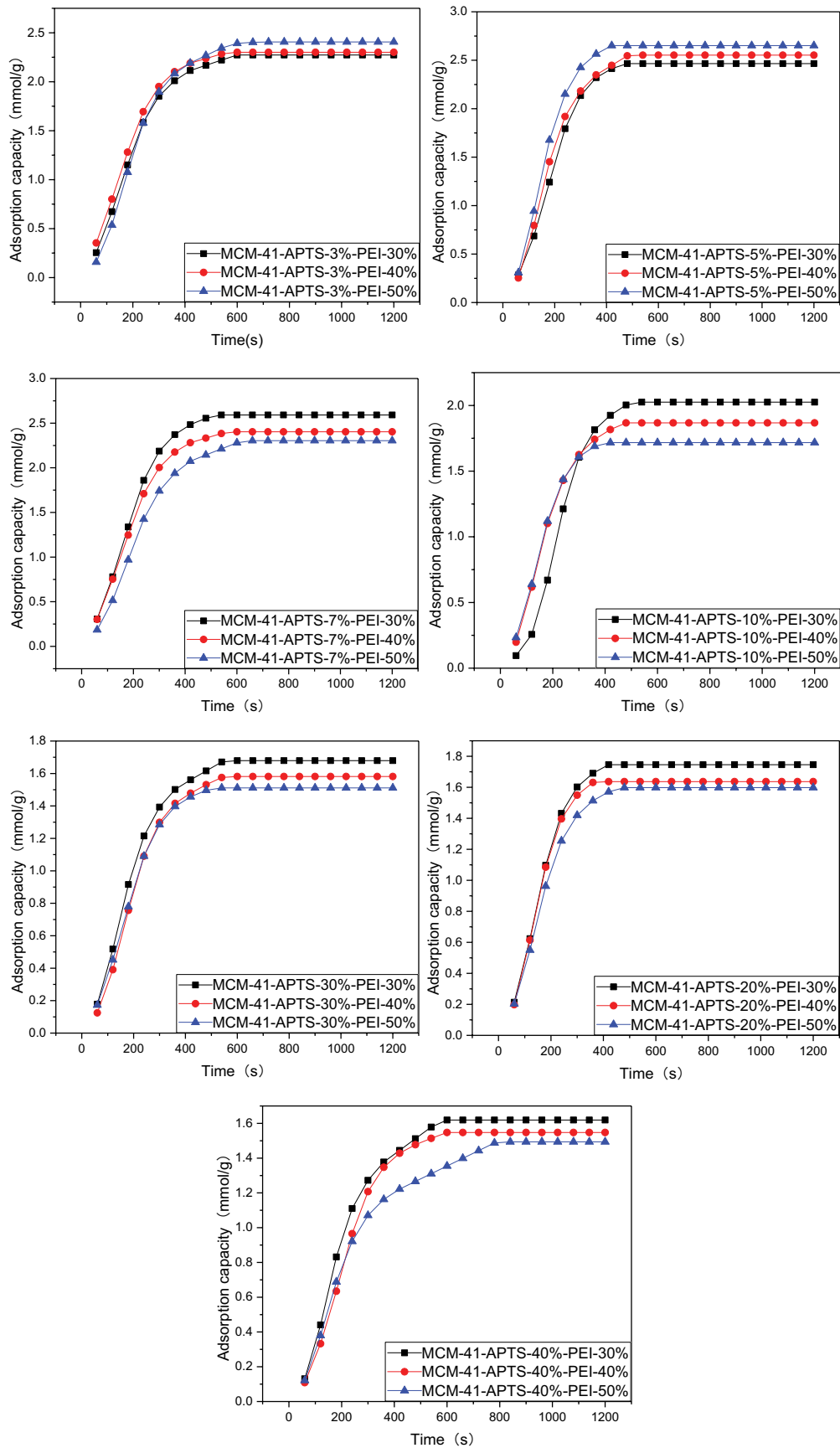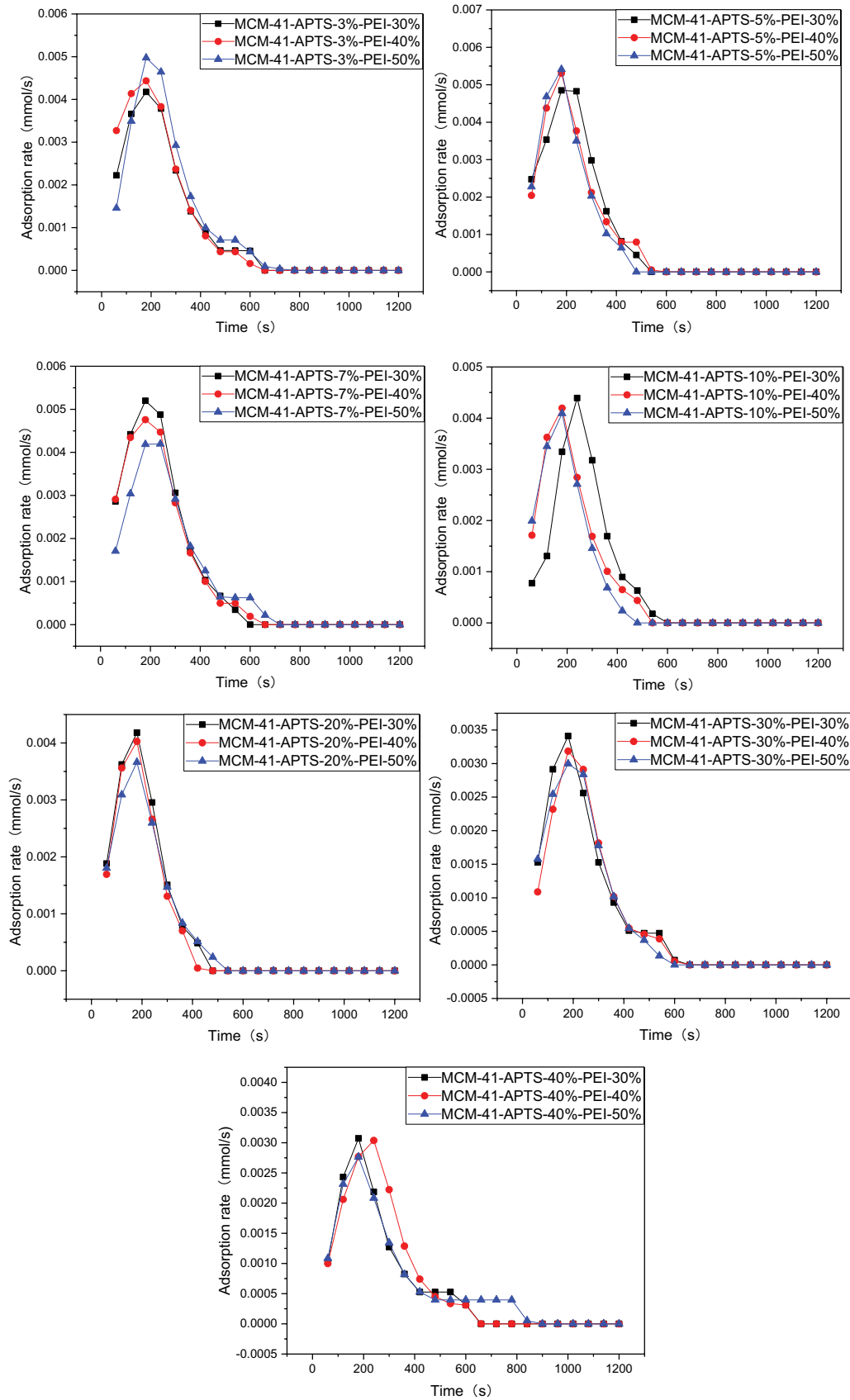
Fig. 4. CO$_2$ adsorption capacities of adsorbents.

Fig. 5. CO_2 adsorption rates of adsorbents

and PEI will reunion in the channel, hinder the diffusion of CO_2 and hinder the amino active site exposure to CO_2, resulting in the decrease of adsorption capacity.

The specific data of CO_2 adsorption capacity of the adsorbents is displayed in Table 2. The adsorbents prepared by the mixture of APTS and PEI showed a good adsorption performance. The maximum CO_2 absorption capacity (2.6512 mmol g^{-1}) was obtained at MCM-41-APTS-5%-PEI-50%. Table 3 shows the comparison of CO_2 adsorption capacity among different adsorbents. It was also higher than waste tea activated carbon (2.48 mmol g^{-1}) [38] and palm shell activated carbon (2.13 mmol g^{-1}) [39] which indicated that modified MCM-41 materials were competitive with other biomass-based porous carbons. APTS is a chain alkanolamine with a steric hindrance group. When grafted

onto the channel surface of MCM-41, it reacts with the silica hydroxyl group on the surface of the carrier and forms a space separation structure in the channel. Meanwhile, duo to high amino density of PEI, when impregnated into the channel of MCM-41-APTS adsorbents, it can be well dispersed and fixed in the channel because of hydrogen bonds generated with the silica-hydroxyl group on the surface of the channel and the amino group in APTS molecules. The space separation structure also can provide a favorable channel for the diffusion of CO_2. Therefore, the synergistic effect of APTS and PEI in the carrier channel improves the CO_2 adsorption performance of the adsorbent.

3.4. Adsorption rate

The CO_2 adsorption rates of MCM-41-APTS-*x*-PEI-*y* adsorbents are shown in Fig. 6. All adsorbents achieved their adsorption equilibrium in 600 s. It was different from the adsorption rate of MCM-41-PEI-*y* which was roughly L-shaped and similar to the results of MCM-41-APTS-x [31], the adsorption rate of MCM-41-APTS-*x*-PEI-*y* adsorbents were first increased rapidly and then decreased gradually. The variation of adsorption rate could be explained

Table 2
CO_2 adsorption capacity

Adsorbents	CO_2 adsorption capacity (mmol g^{-1})
MCM-41-APTS-3%-PEI-30%	2.2733
MCM-41-APTS-3%-PEI-40%	2.3011
MCM-41-APTS-3%-PEI-50%	2.4062
MCM-41-APTS-5%-PEI-30%	2.4652
MCM-41-APTS-5%-PEI-40%	2.5522
MCM-41-APTS-5%-PEI-50%	2.6512
MCM-41-APTS-7%-PEI-30%	2.5917
MCM-41-APTS-7%-PEI-40%	2.4035
MCM-41-APTS-7%-PEI-50%	2.3034
MCM-41-APTS-10%-PEI-30%	2.0254
MCM-41-APTS-10%-PEI-40%	1.8671
MCM-41-APTS-10%-PEI-50%	1.7169
MCM-41-APTS-20%-PEI-30%	1.7456
MCM-41-APTS-20%-PEI-40%	1.6367
MCM-41-APTS-20%-PEI-50%	1.5979
MCM-41-APTS-30%-PEI-30%	1.6795
MCM-41-APTS-30%-PEI-40%	1.5816
MCM-41-APTS-30%-PEI-50%	1.5094
MCM-41-APTS-40%-PEI-30%	1.6191
MCM-41-APTS-40%-PEI-40%	1.5477
MCM-41-APTS-40%-PEI-50%	1.4935

Fig. 6. The cyclic CO_2 adsorption capacity of MCM-41-APTS-5%-PEI-50%.

Table 3
Comparison of CO_2 adsorption capacity among different adsorbents

Adsorbents	CO_2 adsorption capacity (mmol-CO_2/g-sorbent	Reference
MCM-41-APTS-5%-PEI-50%	2.6512	Present study
MCM-41-TEPA60%	2.45	[13]
MCM-41-PEI50%	2.00	[37]
Waste tea activated carbon	2.48	[38]
Palm shell activated carbon	2.13	[39]
Cu(dpt)2(SiF6)]*n*	3.56	[18]
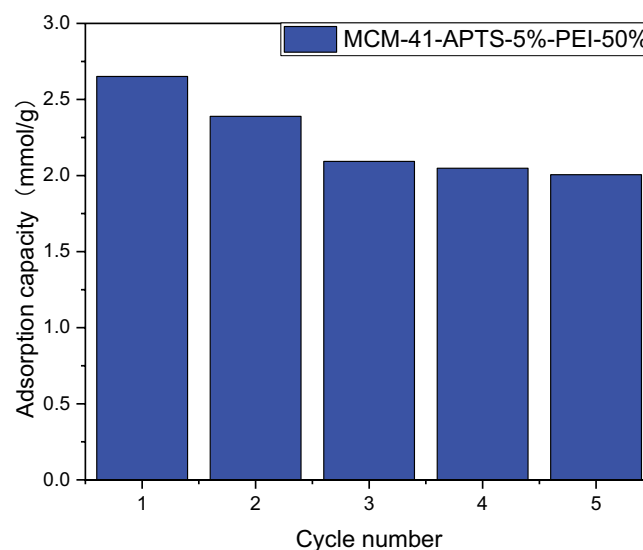
as due to PEI and APTS loading which lead to a physical-chemical adsorption process. Among the modified adsorbents, the maximum adsorption rate was appeared at MCM-41-APTS-5%-PEI-50%.

3.5. Stability of the modified-adsorbents

The recycling performance is an important indicator to evaluate the performance of adsorbents and crucial to the realization of the industrial application. Excellent recycling performance can help reduce the replacement frequency of adsorbent in the production process, improve the utilization rate of adsorbent and reduce the cost of CO_2 capture. Fig. 6 shows the cyclic CO_2 adsorption capacity of MCM-41-APTS-5%-PEI-50%. MCM-41-APTS-5%-PEI-50% displayed a good stability after 5 time recycle. The space steric effect, amidogen of APTS and Si–OH on the surface of carrier made the PEI in the carrier channel well dispersed and firmly fixed which reduced the volatilization of PEI during the regeneration and improved the stability of MCM-41-APTS-5%-PEI-50%.

4. Conclusions

With the increase of APTS and PEI loading rate, the CO_2 adsorption capacity of the adsorbents was first increased and then decreased. When the APTS load rate was 5 wt.% and PEI load rate was 50 wt.%, the maximum CO_2 adsorption capacity of adsorbent (2.6512 mmol g^{-1}) could be obtained, which was 3.53 times of MCM-41. Meanwhile, TGA analysis and CO_2 absorption/desorption isotherms showed that the adsorbent modified by APTS and PEI had better thermal stability and cyclic stability compared with that modified by PEI alone or APTS. After five cycles of CO_2 absorption/desorption, MCM-41-APTS-5%-PEI-50% showed better recycling performance and it was suitable for industrial application.

Acknowledgment

Authorship contribution statement

Z.C (Master)**:** Wrote and revised the manuscript.
Q.C (Associate Professor)**:** Conducted all the experiments and revised the manuscript.

Declaration of interests

The authors declare that they have no known competing financial interests or personal relationships that could have appeared to influence the work reported in this paper.

References

[1] C. Song, Global challenges and strategies for control, conversion and utilization of CO_2 for sustainable development involving energy, catalysis, adsorption and chemical processing, Catal. Today, 115 (2006) 2–32.

[2] S. Babamohammadi, A. Shamiri, M.K. Aroua, A review of CO_2 capture by absorption in ionic liquid-based solvents, Rev. Chem. Eng., 31 (2015), doi: 10.1515/revce-2014-0032.

[3] A. Kiani, K. Jiang, P. Feron, Techno-economic assessment for CO_2 capture from air using a conventional liquid-based absorption process, Front. Energy Res., 8 (2020) 92, doi: 10.3389/fenrg.2020.00092.

[4] F. Ahmad, K.K. Lau, A.M. Shariff, G. Murshid, Process simulation and optimal design of membrane separation system for CO_2 capture from natural gas, Comput. Chem. Eng., 36 (2012) 119–128.

[5] M. Muhammad, Y.F. Yeong, K.K. Lau, A.B.M. Shariff, Issues and challenges in the development of deca-dodecasil 3 rhombohedral membrane in CO_2 capture from natural gas, Sep. Purif. Methods, 44 (2015) 331–340.

[6] D.S. Dao, H. Yamada, K. Yogo, Enhancement of CO_2 adsorption/desorption properties of solid sorbents using tetraethylenepentamine/diethanolamine blends, ACS Omega, 5 (2020) 23533–23541.

[7] M. Alfe, A. Policicchio, L. Lisi, V. Gargiulo, Solid sorbents for CO_2 and CH_4 adsorption: the effect of metal organic framework hybridization with graphene-like layers on the gas sorption capacities at high pressure, Renewable Sustainable Energy Rev., 141 (2021) 110816, doi: 10.1016/j.rser.2021.110816.

[8] Q. Wang, J. Luo, Z. Zhong, A. Borgna, CO_2 capture by solid adsorbents and their applications: current status and new trends, Energy Environ. Sci., 4 (2010) 42–55.

[9] F. Sher, S.Z. Iqbal, S. Albazzaz, U. Ali, D.A. Mortari, T. Rashid, Development of biomass derived highly porous fast adsorbents for post-combustion CO_2 capture, Fuel, 282 (2020) 118506, doi: 10.1016/j.fuel.2020.118506.

[10] E. Davarpanah, M. Armandi, S. Hernández, D. Fino, R. Arletti, S. Bensaid, M. Piumetti, CO_2 capture on natural zeolite clinoptilolite: effect of temperature and role of the adsorption sites, J. Environ. Manage., 275 (2020) 111229, doi: 10.1016/j.jenvman.2020.111229.

[11] T.M. Albayati, A.M. Doyle, Shape-selective adsorption of substituted aniline pollutants from wastewater, Adsorpt. Sci. Technol., 31 (2013) 459–468.

[12] J.-Y. Jung, H.-R. Yu, S.-J. In, Y.C. Choi, Y.-S. Lee, Water vapor adsorption capacity of thermally fluorinated carbon molecular sieves for CO_2 capture, J. Nanomater., 2013 (2013) 705107, doi: 10.1155/2013/705107.

[13] X. Ma, X. Wang, C. Song, "Molecular Basket" sorbents for separation of CO_2 and H_2S from various gas streams, J. Am. Chem. Soc., 131 (2009) 5777–5783.

[14] F. Fashi, A. Ghaemi, P. Moradi, Piperazine-modified activated alumina as a novel promising candidate for CO_2 capture: experimental and modeling, Greenhouse Gases Sci. Technol., 9 (2019) 37–51.

[15] K. Wang, H. Shang, L. Li, X. Yan, Z. Yan, C. Liu, Q. Zha, Efficient CO_2 capture on low-cost silica gel modified by polyethyleneimine, J. Nat. Gas Chem., 21 (2012) 319–323.

[16] J. Wang, Q. Pu, P. Ning, S. Lu, Activated carbon-based composites for capturing CO_2: a review, Greenhouse Gases Sci. Technol., 9 (2021) 377–393.

[17] E.H. Khader, T.J. Mohammed, T.M. Albayati, Comparative performance between rice husk and granular activated carbon for the removal of azo tartrazine dye from aqueous solution, Desal. Water Treat., 229 (2021) 372–383.

[18] H.-M. Wen, C. Liao, L. Li, A. Alsalme, Z.A. Alothman, R. Krishna, H. Wu, W. Zhou, J. Hu, B. Chen, A metal–organic framework with suitable pore size and dual functionalities for highly efficient post-combustion CO_2 capture, J. Mater. Chem. A, 7 (2019) 3128–3134.

[19] K. Kumar, A. Kumar, Enhanced CO_2 adsorption and separation in ionic-liquid-impregnated mesoporous silica MCM-41:

a molecular simulation study, J. Phys. Chem. C, 122 (2018) 8216–8227.

[20] H. Du, L. Ma, X. Liu, F. Zhang, X. Yang, Y. Wu, J. Zhang, A novel mesoporous SiO_2 material with MCM-41 structure from coal gangue: preparation, ethylenediamine modification, and adsorption properties for CO_2 capture, Energy Fuels, 32 (2018) 5374–5385.

[21] T.M. Albayati, S.E. Wilkinson, A.A. Garforth, A.M. Doyle, Heterogeneous alkane reactions over nanoporous catalysts, Transport Porous Media, 104 (2014) 315–333.

[22] T.M. Albayati, A.M. Doyle, Erratum to: encapsulated heterogeneous base catalysts onto SBA-15 nanoporous material as highly active catalysts in the transesterification of sunflower oil to biodiesel, J. Nanopart. Res., 17 (2015) 1–10, doi: 10.1007/s11051-015-2991-8.

[23] T.M. Albayati, I.K. Salih, H.F. Alazzawi, Synthesis and characterization of a modified surface of SBA-15 mesoporous silica for a chloramphenicol drug delivery system, Heliyon, 5 (2019) e02539, doi: 10.1016/j.heliyon.2019.e02539.

[24] S.M. Alardhi, T.M. Albayati, J.M. Alrubaye, A hybrid adsorption membrane process for removal of dye from synthetic and actual wastewater, Chem. Eng. Process. Process Intensif., 157 (2020) 108113, doi: 10.1016/j.cep.2020.108113.

[25] S.M. Alardhi, J.M. Alrubaye, T.M. Albayati, Adsorption of Methyl Green dye onto MCM-41: equilibrium, kinetics and thermodynamic studies, Desal. Water Treat., 179 (2020) 323–331.

[26] S. Reiser, M. Türk, Influence of temperature and high-pressure on the adsorption behavior of sc CO_2 on MCM-41 and SBA-15, J. Supercrit. Fluids, 144 (2019) 122–133.

[27] A. Sharma, J. Jindal, A. Mittal, K. Kumari, N. Kumar, Carbon materials as CO_2 adsorbents: a review, Environ. Chem. Lett., 19 (2021), doi: 10.1007/s10311-020-01153-z.

[28] D. Bahamon, W. Anlu, S. Builes, M. Khaleel, L.F. Vega, Effect of amine functionalization of MOF adsorbents for enhanced CO_2 capture and separation: a molecular simulation study, Front. Chem., 8 (2021), doi: 10.3389/fchem.2020.574622.

[29] J.W. Wei., L. Liao, Y. Xiao, P. Zhang, Y. Shi, Capture of carbon dioxide by amine-impregnated as-synthesized MCM-41, J. Environ. Sci., 22 (2010) 1558–1563.

[30] Z.-L. Liu, Y. Teng, K. Zhang, Y. Cao, W.-P. Pan, CO_2 adsorption properties and thermal stability of different amine-impregnated MCM-41 materials, J. Fuel Chem. Technol., 41 (2013) 469–475.

[31] N. Rao, M. Wang, Z.M. Shang, Y.W. Hou, G.Z. Fan, J.F. Li, CO_2 adsorption by amine-functionalized MCM-41: a comparison between impregnation and grafting modification methods, Energy Fuels, 32 (2017) 670–677.

[32] S. Kim, J. Ida, V.V. Guliants, J.Y.S. Lin, Tailoring pore properties of MCM-48 silica for selective adsorption of CO_2, J. Phys. Chem. B, 109 (2005) 6287–6293.

[33] H.Y. Huang, R.T. Yang, D. Chinn, C.L. Munson, Amine-grafted MCM-48 and silica xerogel as superior sorbents for acidic gas removal from natural gas, Ind. Eng. Chem. Res., 42 (2003) 2427–2433.

[34] X. Wang, L. Chen, Q. Guo, Development of hybrid amine-functionalized MCM-41 sorbents for CO_2 capture, Chem. Eng. J., 260 (2015) 573–581.

[35] H.L. Zhao, J. Hu, J.J. Wang, L.H. Zhou, H.L. Liu, CO_2 capture by the amine-modified mesoporous materials, Acta Phys. Chim. Sin., 23 (2007) 801–806.

[36] J. Wang, H. Chen, H. Zhou, X. Liu, W. Qiao, D. Long, L. Ling, Carbon dioxide capture using polyethylenimine-loaded mesoporous carbon, J. Environ. Sci., 25 (2013) 124–132.

[37] X. Wang, X. Ma, C. Song, D.R. Locke, S. Siefert, R.E. Winans, J. Möllmer, M. Lange, A. Möller, R. Gläser, Molecular basket sorbents polyethylenimine–SBA-15 for CO_2 capture from flue gas: characterization and sorption properties, Microporous Mesoporous Mater., 169 (2013) 103–111.

[38] S. Rattanaphan, T. Rungrotmongkol, P. Kongsune, Biogas improving by adsorption of CO_2 on modified waste tea activated carbon, Renewable Energy, 145 (2020) 622–631.

[39] N.A. Rashidi, S. Yusup, Potential of palm kernel shell as activated carbon precursors through single stage activation technique for carbon dioxide adsorption, J. Cleaner Prod., 168 (2017) 474–486.